Journal of Engineering and Computer Sciences
Qassim University, Vol. 10, No. 1, pp. 19-38 (January 2017/Rabi' II 1438H)

The Effect of Cooling Medium on the Temperature of High-Concentrating Multi-Junction Solar Cells using Non-uniform Incident Light

Fahad G. Al-Amri

fgalamri@uod.edu.sa

Department of Basic Engineering, College of Engineering, University of Dammam, P.O. Box 1982, Dammam 31441, Saudi Arabia

(Received 16/10/2016; Accepted for Publication 1/12/2016)

Abstract. A numerical model of heat transfer for predicting solar cell temperature in a high concentrating photovoltaic module using non-uniform incident illumination is presented. The PV module, based on a three-junction solar cell with a front contact to the cell, anti-reflected glass coating, and an active aluminum back plate is modeled. The Gaussian distribution is adopted to simulate the irregularity in the incident radiation. The cooling water is enforced to flow inside a rectangular duct behind the solar cell assembly to lower the cell's operating temperature. The continuity equation, momentum equation, energy equation for the fluid, and energy equations for the solid materials in the solar cell assembly are solved using a numerical marching technique. The effects of the standard deviation of light distribution, position of the maximum radiation on the cell surface, Reynold's number, and concentration ratio on the temperature of the solar cell are illustrated. At moderate values of concentration ratio, water was found to be an effective cooling medium in reducing solar cell temperatures to acceptable levels. However, for high concentrations, plain water-cooling system was unable to cool the solar cell adequately when the system is subjected to a sharp non-uniform illumination distribution.

***Keywords**:* triple-junction solar cell; irregular incident light; conjugate heat transfer

Nomenclature

b	channel width, m
C	concentration ratio
Gr^*	modified Grashof number, $\frac{g\beta q_{avg} b^4}{\upsilon^2 K_f}$
I	intensity of incident light, W/m^2
k	thermal conductivity, $W/m \cdot K$
ℓ	channel length, m

L dimensionless plate length, $\frac{\ell}{b\,\mathrm{Re}}$

p pressure of fluid at any cross section, N/m^2

p' pressure defect at any cross section, $p-p_s$, N/m^2

p_s hydrostatic pressure, $-\rho_\infty gz$, N/m^2

p_∞ pressure of fluid at the channel entrance, N/m^2

P dimensionless pressure at any cross section, $\frac{p'-p_\infty}{\rho_\infty u_\infty^2}$

q_{avg} average input heat flux, $(1-\eta)\,I_{avg}$ W/m^2

Re Reynolds number, $\frac{u_o b}{\upsilon}$

t solar cell assembly thickness, m

T temperature at any point, K

T_∞ inlet temperature, K

SD standard deviation

u_∞ entrance axial velocity, m/s

u longitudinal velocity component at any point, m/s

U dimensionless longitudinal velocity, u/u_∞

v transverse velocity component at any point, m/s

V dimensionless transverse velocity, b * v / υ

y horizontal coordinate, m

Y dimensionless horizontal coordinate, y / b

z vertical coordinate, m

z_0 position of the maximum incident light, m

Z dimensionless vertical coordinate, z / (b * Re)

Greek Symbols

υ kinematic fluid viscosity

ρ fluid density, kg/m^3

μ dynamic fluid viscosity, $kg/m\cdot s$

α absorptivity

η efficiency of the solar cell

θ dimensionless temperature at any point, $\left[\frac{k_f T}{q_{avg} b}\right]$

θ_∞ dimensionless inlet temperature at any point, $\left[\frac{k_f T_\infty}{q_{avg} b}\right]$

Subscripts

ad adhesive material

c	a Cu-Ag-Hg front contact
e	exit
f	fluid
g	glass
s	solid
w	wall of the channel
∞	ambient or inlet
1	duct wall at Y = 0
2	duct wall at Y = 1

1. Introduction

Energy is increasingly important in engineering problems, and researchers have devoted much effort toward developing modern techniques to reduce the cost of its production. Concentrating multi-junction photovoltaics represent an emerging technology that aspires to produce a major amount of the global energy demand. However, studies have shown that the performance of a photovoltaic system is largely dependent on the cell temperature, and its efficiency is reduced with a negative temperature coefficient. In addition, as a result of using an optical concentrator, the incident illumination on the solar cell is strongly non-uniform, increasing cell temperatures. Therefore, maintaining solar cell performance requires cooling, and it can be either active or passive.

Several studies have investigated the thermal behavior of a CPV. A theoretical thermal model was developed by Cui Min *et al.* [1] and Cotal and Frost [2] for simulating the thermal performance of a solar cell under natural convection heat transfer. Vicenza *et al.* [3] used an active cooling system consisting of micro channels directly beneath the cells through which water circulates. Moshfegh and Sandberg [4] carried out both numerical and experimental studies of free convection heat transfer behind solar cells. The performance of hybrid photovoltaic/thermal (PV/T) solar systems was evaluated by several researchers [5,6,7]. Al-Amri and Mallick [8,9] presented a thermal model for predicting the maximum cell temperatures in multi-junction concentrating solar cell systems that were actively cooled by water-forced and air-forced convection. The thermal performance was found to be substantially dependent on the geometrical parameters. Micheli *et al.* [10] recently presented a thorough review of micro- and nano-technologies that apply to CPV cooling and associated manufacturing technologies. Carbon nano-tubes and high-conductive coating technologies are reportedly the most effective at CPV cooling.

The non-uniform illumination profiles problem has been studied extensively, focusing on the effects of non-uniformity on electrical performance [11]. However, some research has addressed the thermal impacts of non-uniformity in radiation shapes. Franklin and Conventry [12] showed, in their numerical and experimental study, that there is a drop in both open-circuit voltage and efficiency in a silicon solar

cell under non-uniform focused illumination, compared to a cell under uniform illumination. In addition, results indicated that the temperature profile closely resembles a Gaussian distribution. Conventry *et al.* [13] measured the thermal and electrical output from a concentrating PV/thermal collector at 25-30 suns. They found that the illumination flux intensity across the width of the solar cell was far from even. Domenech-Garret [14] investigated the effects of a combination of non-uniform illumination and non-uniform temperature on a silicon solar cell using Gaussian and inverse Gaussian profiles to describe the temperature in the cell. Chemisana and Rosell [15] studied, both numerically and experimentally, the effects of Gaussian and anti-Gaussian temperature profiles on the cell's electrical parameters under various types of concentrated illumination. Electric conversion efficiency increased under a Gaussian temperature profile and decreased when the cell was subjected to an inverse Gaussian temperature curve. The authors concluded that the temperature profile could be tailored to maximize efficiency for specific radiation conditions. Al-Amri and Mallick [16] studied the effects of combined radiation and air-forced convection on the concentrating triple-junction solar cell temperature under non-uniform illumination and found that surface radiation exchange inside the duct reduced the cell's maximum temperature. However, results showed that their cooling system was suitable only at low concentrations (C<100). Recently, Xing *et al.* [17] investigated the thermal and electrical performances of a silicon vertical multi-junction solar cell under non-uniform radiation, revealing a noticeable increment in cell temperature as the degree of non-uninformity was increased.

A thorough literature review reveals that the effects of non-uniform incident light on the operating temperature of solar cells is yet to be well understood. The feature of non-uniformity, and therefore its impact on the solar cell temperature, is worthy of additional consideration and forms the focus of this work. Thus, the aim of the present work is to extend the work of Al-Amri and Mallick [16] by using water, instead of air, as a coolant medium to actively cool highly-concentrated solar cell under non-uniform incident light. The effect of using different cooling mediums will be explored, and a comparison between solar cell temperatures of the present results and those obtained for active air cooling by Al-Amri and Mallick [16] will be presented and discussed.

A numerical model of heat transfer was employed to simulate the temperature distribution, under the non-uniform incident light, on highly-concentrated triple-junction solar cells.

2. Mathematical Formulations

Fig. 1 shows the geometry of the physical problem and the coordinate system considered in this study. The components consisted of a solar cell with three p-n junctions made of galium indium phosphide (GaInP), galium arsenide (GaAs), and germanium (Ge), a Cu-Ag-Hg frontal contact to the cell, a front glass coating, a rear aluminum plate, and a sticky material used to attach the cell to the coating glass and

the aluminum plate. The cooling water flows through channel behind the aluminum plate, which its external plate was assumed to be adiabatic. The inlet temperature of the fluid was assumed to be constant at T_{∞}=27°C. The efficiency of the solar cell (η) and the optical system (η_{opt}) were 0.38 and 0.85, respectively. The dimensions and the thermo-physical properties of the components used in the model can be found in [16].

The illumination distribution incident on the solar cell surface was assumed to be non-uniform and in the shape of a Gaussian profile [12], where its formula can be written as:

$$I(z)=\frac{2C}{10^4\,SD\sqrt{2\pi}}\,e^{\frac{-2(z-z_0)^2}{SD^2}} \tag{1}$$

where z_0 is the position of the maximum illumination on the cell surface, C is the concentration ratio, and SD is the standard deviation measuring how far incident illumination is dispersed.

The intensity of the incident light, I(z), can be written in a non-dimensional form as:

$$\bar{I}(Z)=\frac{I(z)}{I_{avg}} \tag{2}$$

where I_{avg} is the average incident illumination across the entire cell surface.

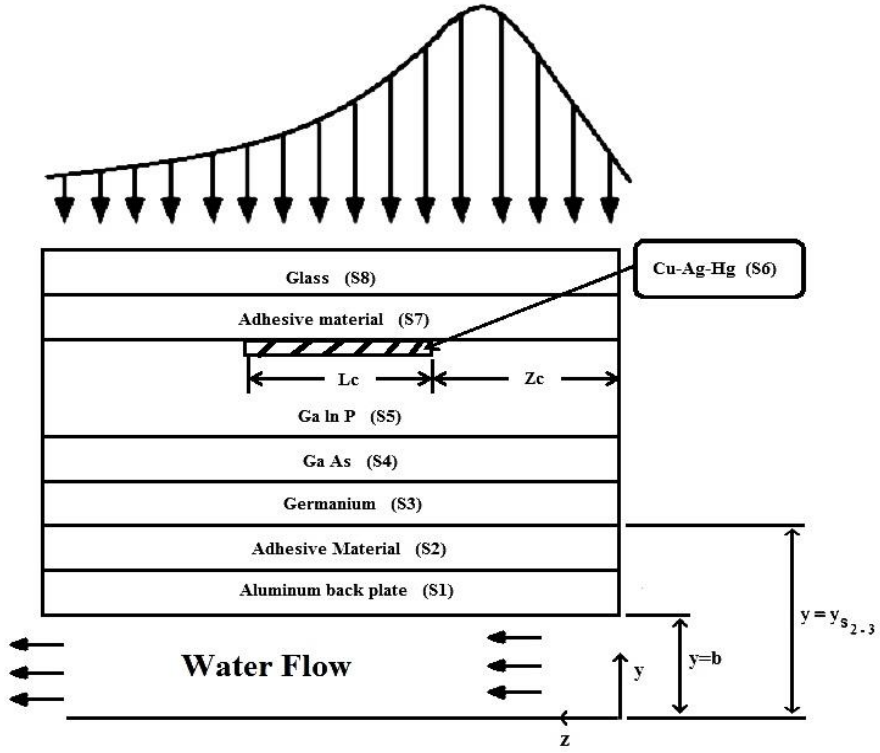

Fig. (1). Geometry of the employed system

The equations governing the physical problem under consideration can be expressed as the following [9]:

$$\frac{\partial V}{\partial Y}+\frac{\partial U}{\partial Z}=0 \tag{3}$$

$$V\frac{\partial U}{\partial Y}+U\frac{\partial U}{\partial Z}=\frac{dP}{dZ}+\frac{G_r^*}{Re}\left(\theta-\theta_\infty\right)+\frac{\partial^2 U}{\partial Y^2} \tag{4}$$

$$V\frac{\partial \theta_f}{\partial Y}+U\frac{\partial \theta_f}{\partial Z}=\frac{1}{Pr}\frac{\partial^2 \theta_f}{\partial Y^2} \tag{5}$$

$$\frac{\partial^2 \theta_s}{\partial Y^2}=0 \tag{6}$$

The continuity equation, Eq. (3), can be written in its integral form as:

$$F = \int_0^1 U dY = 1 \tag{7}$$

The boundary conditions of the above equations are:

At channel entrance (Z = 0):

$$U=1,\ V = P = 0, \text{ and } \theta = \theta_\infty \tag{8a}$$

At the first wall of the channel (Y = 0):

$$U = 0,\ V = 0 \text{ and } \left.\frac{\partial \theta_f}{\partial Y}\right|_{Y=0} = 0 \tag{8b}$$

At the second wall of the channel (Y = 1):

$$U = 0,\ V = 0 \text{ and } Kr_{s_1-f} \left.\frac{\partial \theta_s}{\partial Y}\right|_{Y=1^+} = \left.\frac{\partial \theta_f}{\partial Y}\right|_{Y=1^-} \tag{8c}$$

At solid-solid interfaces:

At $Y = Y_{S_{(j)-(j+1)}}$, and j = 1 or 2,

$$\left.\frac{\partial \theta_s}{\partial Y}\right|_{Y=Y^-_{S_{(j)-(j+1)}}} = kr_{S_{(j+1)-(j)}} \left.\frac{\partial \theta_s}{\partial Y}\right|_{Y=Y^+_{S_{(j)-(j+1)}}} \tag{8d}$$

For $Y = Y_{S_{(j)-(j+1)}}$, $0 < Z < Z_c$ or $(Z_c+L_c) < Z < L$, and j = 3 or 4,

$$\left.\frac{\partial \theta_s}{\partial Y}\right|_{Y=Y^-_{S_{(j)-(j+1)}}} = kr_{S_{(j+1)-(j)}} \left.\frac{\partial \theta_s}{\partial Y}\right|_{Y=Y^+_{S_{(j)-(j+1)}}} + \frac{(1-\eta)\alpha_{s_i}(1-\alpha_g-\alpha_{ad})\,\bar{I}(Z)}{Kr_{S_j-f}} \tag{8e}$$

For $Y = Y_{S_{5-7}}$ and $0 < Z < Z_c$ or $(Z_c+L_c) < Z < L$,

$$\left.\frac{\partial \theta_s}{\partial Y}\right|_{Y=Y^-_{S_{5-7}}} = kr_{S_{7-5}} \left.\frac{\partial \theta_s}{\partial Y}\right|_{Y=Y^+_{S_{5-7}}} + \frac{(1-\eta)\alpha_{s_5}(1-\alpha_g-\alpha_{ad})\,\bar{I}(Z)}{Kr_{S_5-f}} \tag{8f}$$

At $Y = Y_{S_{(j)-(j+1)}}$, $Z_c \le Z \le (Z_c + L_c)$, and j = 3, 4, or 5,

$$\left.\frac{\partial \theta}{\partial Y}\right|_{Y=Y^-_{S_{(j)-(j+1)}}} = kr_{S_{(j+1)-(j)}} \left.\frac{\partial \theta}{\partial Y}\right|_{Y=Y^+_{S_{(j)-(j+1)}}} \tag{8g}$$

At $Y = Y_{S_{6-7}}$ and $Z_c \le Z \le (Z_c + L_c)$,

$$\left.\frac{\partial\theta}{\partial Y}\right|_{Y=Y^{-}_{S_{6-7}}} = kr_{S_{7-6}} \left.\frac{\partial\theta}{\partial Y}\right|_{Y=Y^{+}_{S_{6-7}}} + \frac{\alpha_{s_6}(1-\alpha_g-\alpha_{ad})\,\bar{I}(Z)}{kr_{S_6-f}} \tag{8h}$$

At $Y = Y_{S_{7-8}}$,

$$\left.\frac{\partial\theta}{\partial Y}\right|_{Y=Y^{-}_{S_{7-8}}} = kr_{S_{8-7}} \left.\frac{\partial\theta}{\partial Y}\right|_{Y=Y^{+}_{S_{7-8}}} + \frac{\alpha_{s_7}(1-\alpha_g-\alpha_{ad})\,\bar{I}(Z)}{kr_{S_7-f}} \tag{8i}$$

At $Y = Y_{S_8}$,

$$\left.\frac{\partial\theta}{\partial Y}\right|_{Y=Y_{S_8}} = \frac{\alpha_g\,\bar{I}(Z)}{kr_{S_8-f}} \tag{8j}$$

Where $kr_{S_{(j+1)-j}} = \dfrac{k_{S_{j+1}}}{k_{s_j}}$ and $kr_{S_j-f} = \dfrac{k_{S_j}}{k_f}$

Method of Solution

The conjugate convection field equations (*i.e.*, continuity, momentum, and energy) and the corresponding boundary conditions were transformed into finite difference equations. These equations were then solved using a numerical marching technique. The details of the solution procedure can be found in Coney and El-Shaarawi [18], and the validation of the numerical code can be found in Al-Amri and El-Shaarawi [19].

3. Results and Discussion

The incident illumination profiles obtained using C = 400 and η_{opt} = 0.85 in Eq. (1) are shown in Figs. 2(a) and 2(b) at selected values for SD (0.0005, 0.001, and 0.002) and position of maximum illumination on the cell surface (z_0= 2, 5, and 8 mm), respectively. The uniform incident light profile is shown in Fig. 2(a) for comparative purposes. These profiles were used as code input data so that the effects of these parameters on the temperature distribution of the solar cell could be studied.

To investigate the effect of using different cooling mediums on solar cell temperatures, a comparison between solar cell temperatures of the present results which used water as a cooling medium and those for active air cooling of Al-Amri and Mallick [16] is carried out, for C=100, as shown in Figures 3 and 4 for different values of Reynold's number and different standard deviation values, respectively. It is clear that there is a huge drop in solar cell temperatures when the air is replaced by water. These two figures indicate that air is inappropriate coolant medium at

medium concentration ratios. In contrast, water is an excellent coolant medium at these levels of concentration, and can also be efficient at higher C values as will be shown further on in this paper.

Figs. 5(a), 5(b), and 5(c) show, for z_0 = 5 mm and Re = 500, the variations in solar cell temperature with the axial distance from the channel entrance for both uniform and non-uniform incident light for three selected values of concentration ratio (C) namely, 100, 200, and 400 respectively. Results show that when distribution is uniform, the solar cell temperature first increases sharply near the entrance and then gradually increases until reaching its maximum value at the channel exit. On the other hand, when the distribution is non-uniform, the temperature of the first quarter of the solar cell remains constant at ambient temperature, then rapidly increases to its maximum value at the center of the cell. The temperature then drops sharply and gradually in the fourth quarter of the solar cell, where temperatures are higher than those observed in the first quarter. The figures show that the temperature profile becomes thinner, and the maximum temperature increases, as the SD decreases. Also, the maximum temperature of the solar cell is much higher when the light distribution is non-uniform rather than uniform. Moreover, the effect of the non-uniformity on the solar cell temperature increases with increasing concentration ratio. For example, as the incident light distribution shifted from uniform to non-uniform at SD = 0.0005, the maximum solar cell temperature is shown to increase from 38°C to 88.6°C (*i.e.*, by 133%) and from 71°C to 273°C (*i.e.*, by 284%) when C is 100 and 400, respectively. From another view point, as C increased from 100 to 400, the maximum solar cell temperature increased from 38°C to 71°C (*i.e.*, by 87%) for uniform light distribution, but it increased from 88.6°C to 273°C (*i.e.*, by 208%) for non-uniform distribution at this SD. More importantly, these figures indicate that water can be a proper medium to cool modern multi-junction solar cells up to C=200 and C=400 for strong and mild non-uniform light distributions, respectively.

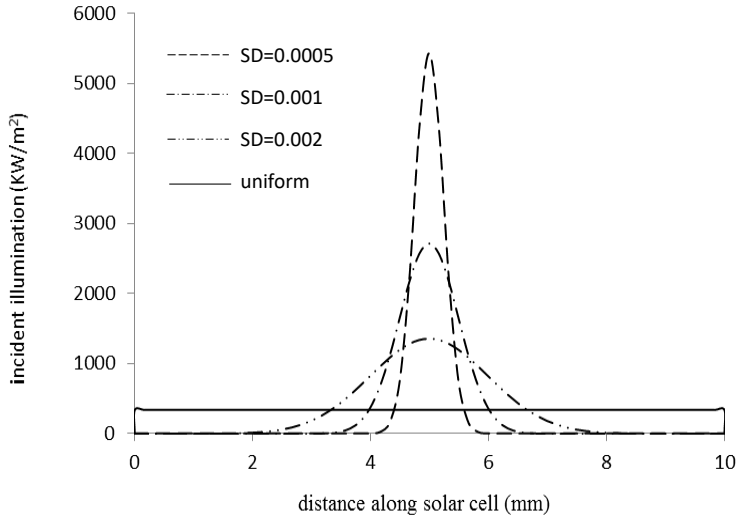

(a)

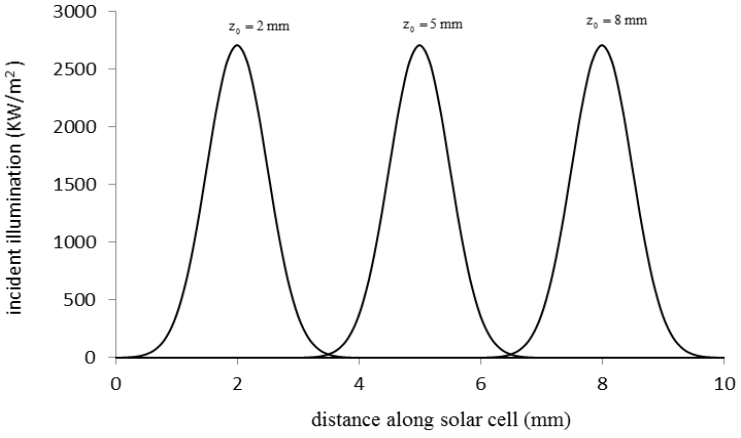

(b)

Fig. (2). Incident illumination profiles for C = 400 and η_{opt} = 0.85 at (a) various SDs and (b) various values of z_0.

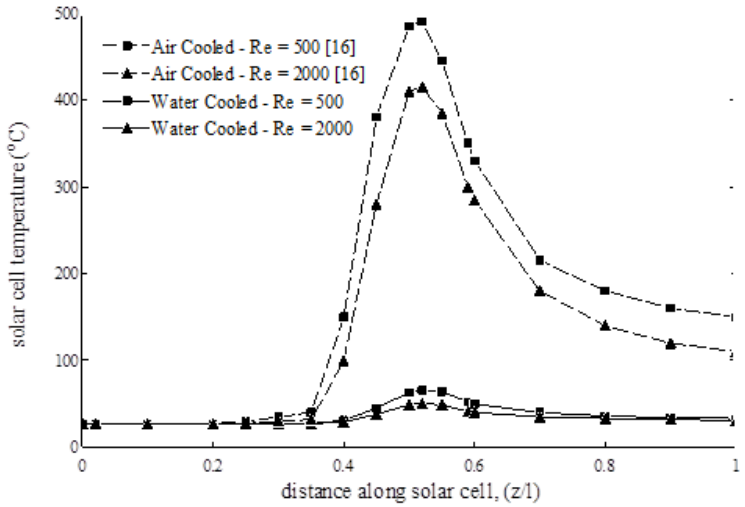

Fig. (3). Comparison of solar cell temperatures when water and air are used as cooling medium using various values of Re when z_0= 0.5, SD=0.001, and C = 100.

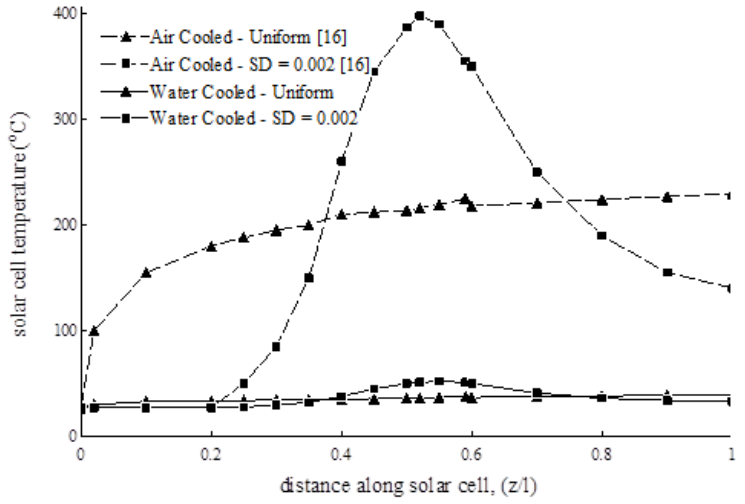

Fig. (4). Comparison of solar cell temperatures when water and air are used as cooling medium for uniform and non-uniform radiation distribution when z_0= 0.5, Re=500, and C = 100.

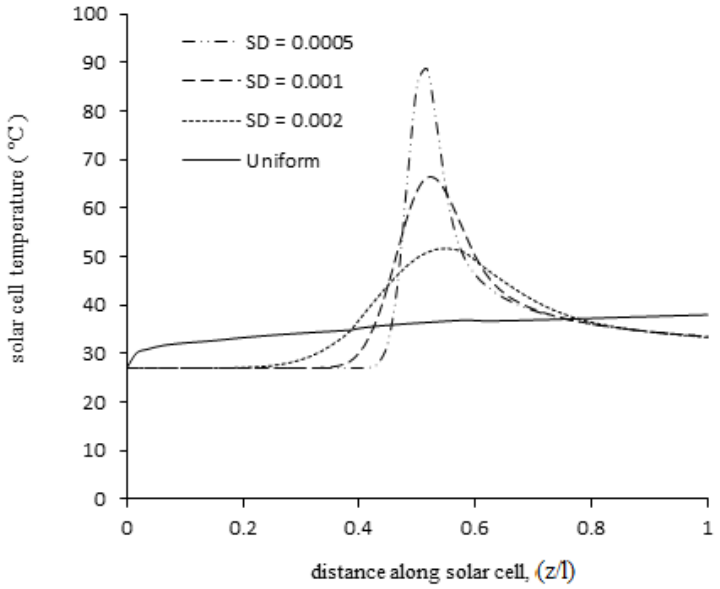

Fig. 5(a). Variation in solar cell temperature using various values of SD when z_0= 0.5, Re = 500, and C = 100.

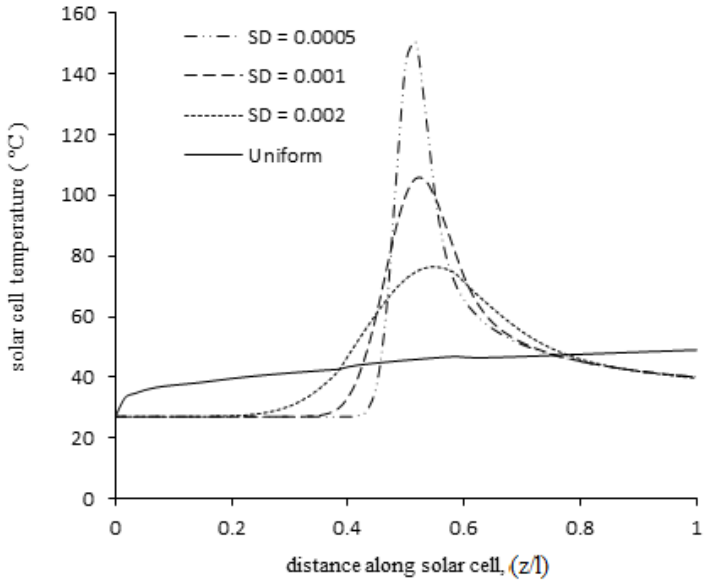

Fig. 5(b). Variation in solar cell temperature using various values of SD when z_0= 0.5, Re = 500, and C = 200.

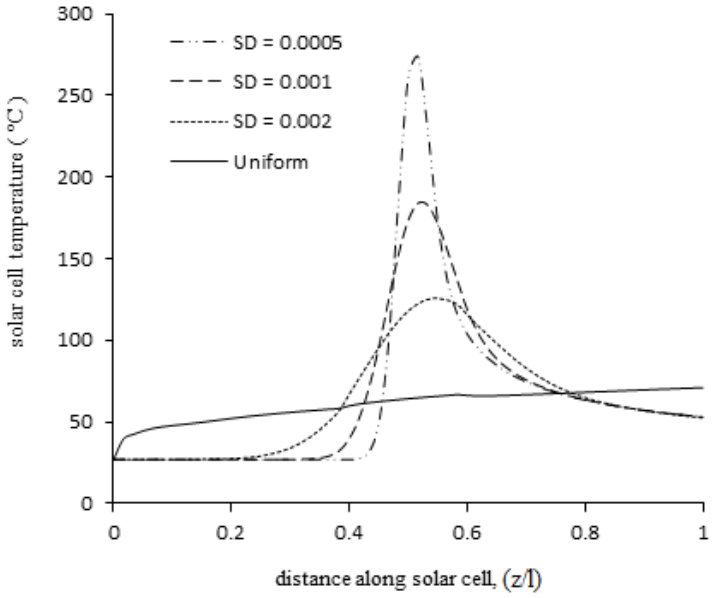

Fig. 5(c). Variation in solar cell temperature using various values of SD when z_0= 0.5, Re = 500, and C = 400.

Figs. 6(a), 6(b), and 6(c) show, for z_0 = 5 mm, Re = 1000, and selected values of SD (0.0005, 0.001, and 0.002), how solar cell temperature varies with axial distance from the channel entrance for both uniform and non-uniform incident light when C= 100, 200, and 400, respectively. Likewise, Figs. 7(a), 7(b), and 7(c) show the same phenomenon when Re = 2000. An obvious reduction in the maximum cell temperature as Re increases can be observed from these figures. The effect of Re on the maximum temperature is more pronounced when the incident light profile is non-uniform than when it is uniform. As seen in Figs. 6 and 7, the maximum solar cell temperature falls down from 71°C to 54°C (*i.e.*, by 24%) as Re increases from 500 to 2000 when the profile is uniform but from 273°C to 171°C (*i.e.*, by 37%) when the profile is non-uniform.

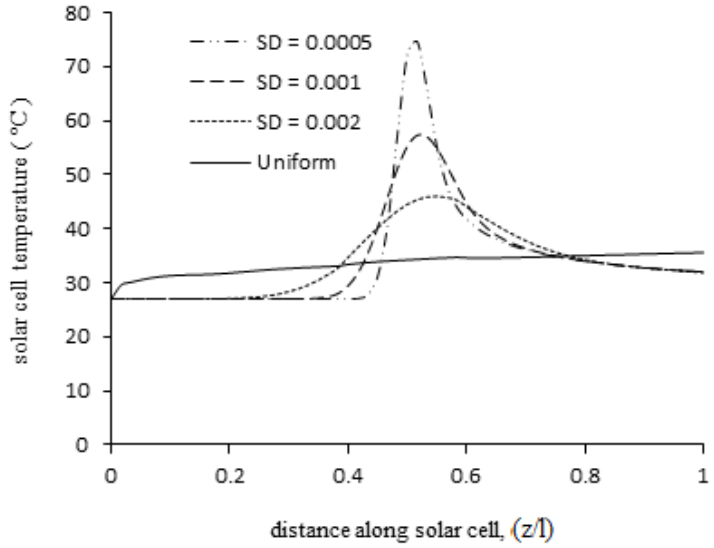

Fig. 6(a). Variation in solar cell temperature using various values of SD when z_0= 0.5, Re = 1000, and C = 100.

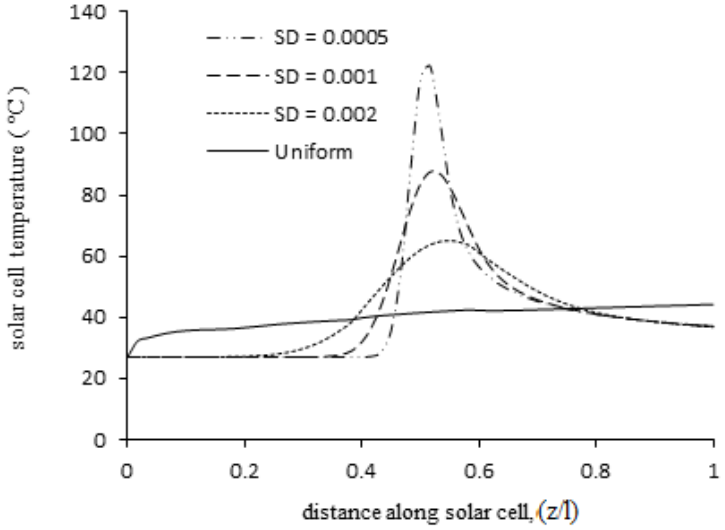

Fig. 6(b). Variation in solar cell temperature using various values of SD when z_0= 0.5, Re = 1000, and C = 200.

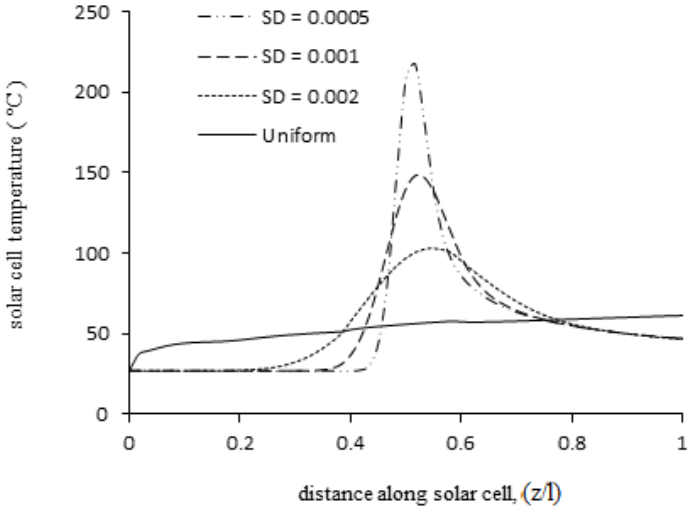

Fig. 6(c). Variation in solar cell temperature using various values of SD when z_0= 0.5, Re = 1000, and C = 400.

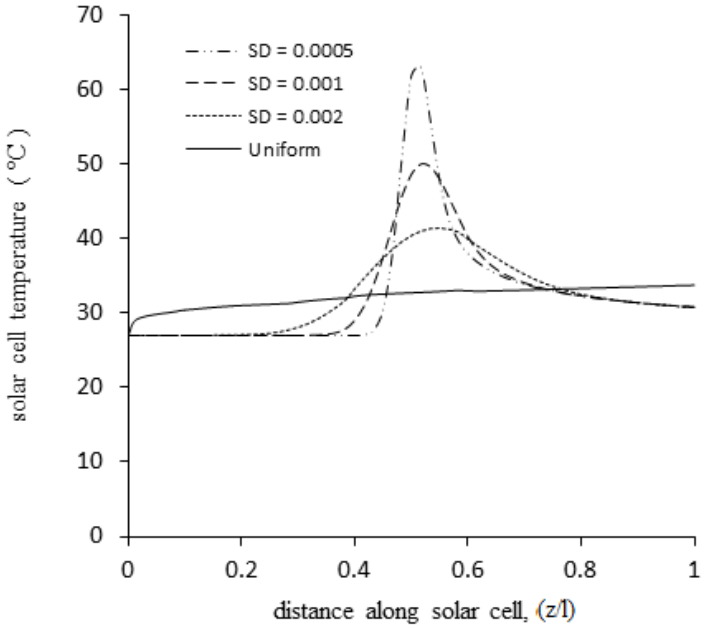

Fig. 7(a). Variation in solar cell temperature using various values of SD when z_0= 0.5, Re = 2000, and C = 100.

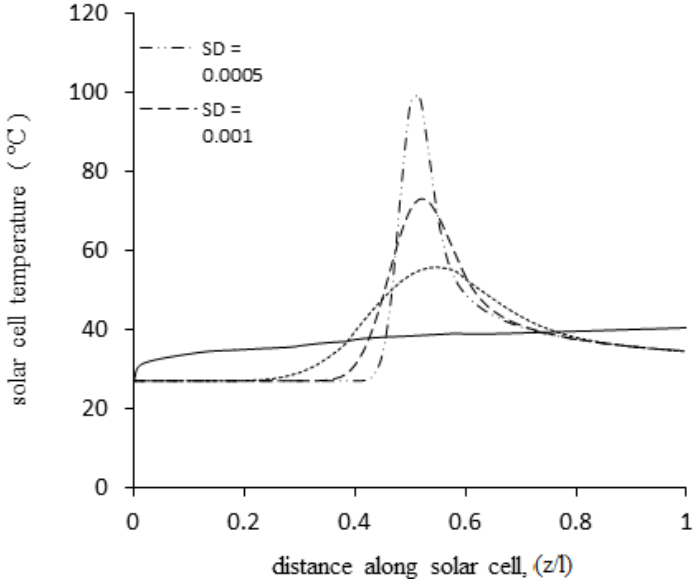

Fig. 7(b). Variation in solar cell temperature using various values of SD when z_0= 0.5, Re = 2000, and C = 200.

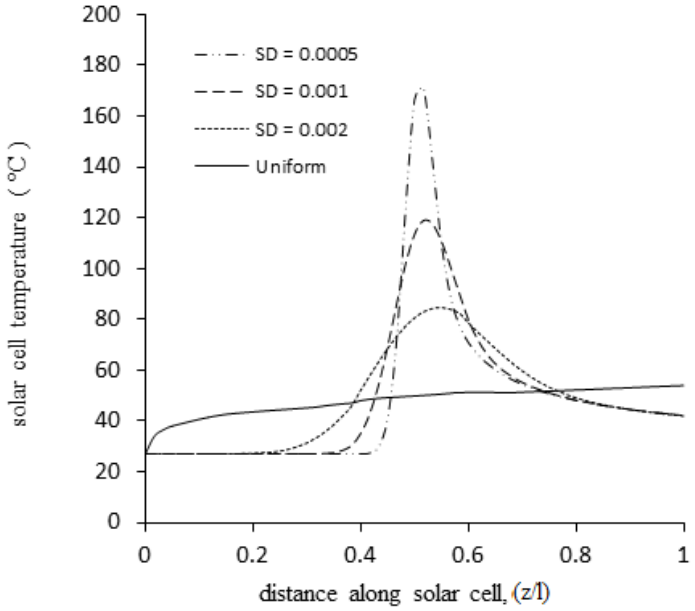

Fig. 7(c). Variation in solar cell temperature using various values of SD when z_0= 0.5, Re = 2000, and C = 400.

The effect of the position of maximum incident light on the solar cell temperature distribution is shown in Fig. 8. A hot spot formed on the portion of the cell surface that was exposed to a large amount of light. This spot became more pronounced when the maximum incident light was at the center of the cell (because of the presence of contact metal), and it was slightly less pronounced when the position was near the leading edge (because of high convective heat transfer near the entrance of the channel).

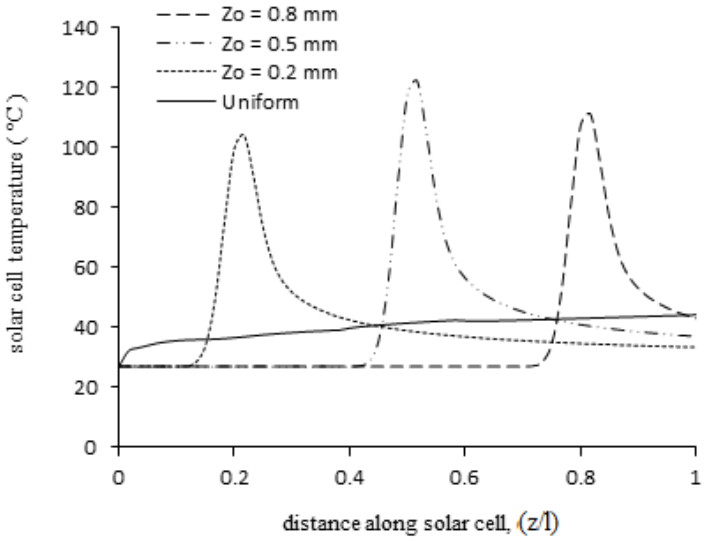

Fig. (8). Variation in solar cell temperature using various values of z_0 when SD = 0.0005, Re = 100, and C = 200

4. Conclusions

The effects of active water cooling on the temperature of a high-concentrating triple-junction solar cell under non-uniformity of incident radiation were modeled. Non-uniformity was simulated using a Gaussian distribution and was found to drastically change the temperature distribution of the solar cell, causing hot spots in some parts of the cell surface. The effect of non-uniformity increases as the concentration ratio increases, and it decreases as either the Reynolds number or standard deviation increases. Moreover, contrary to the case of active air cooling, water cooling was found to be a useful tool for removing heat from solar cell at moderate concentrations. Nevertheless, the conventional water cooling system was inadequate at cooling the solar cell at high concentration ratios ($C \geq 400$) under sharp non-uniform illumination distribution, even when Re was high (up to 2000). Therefore, to improve the performance of such photovoltaic systems, it will be necessary to

redistribute the incident light on the cell surface to alleviate non-uniformity or to use more effective cooling systems.

References

[1] Min, C., Nuofu, C., Xiaoli, Y., Yu, W., Yiming, B. and Xingwang, Z. "Thermal Analysis and Test for Single Concentrator Solar Cells," Journal of Semiconductors, Vol. 30, No. 4, (2009), pp. 1-4.

[2] Cotal, H. and Frost, J. "Heat Transfer Modeling of Concentrator Multijunction Solar Cell Assemblies using Finite Difference Techniques," 31st IEEE PVSC Conference, (2010), pp. 213-218.

[3] Vincenzi, D., Bizzi, F., Stefancich, M., Malagu, C., Morini, G. L., Antonini, A. and Martinelli, G. "Micromachined Silicon Heat Exchanger for Water Cooling of Concentrator Solar Cell," Conference record, PV in Europe Conference and Exhibition-From PV technology to Energy Solutions, (2002), pp. 7-11, Rome, Italy.

[4] Moshfegh, B. and Sandberg, M. "Flow and Heat Transfer in the Air Gap Behind Photovoltaic Panels," Renewable and Sustainable Energy Reviews, Vol. 2, (1998), pp. 287-301.

[5] Bhargava, A. K., Garg, H. P. and Agarwal, R. K. "A Study of a Hybrid Solar System-solar Air Heater Combined with Solar Cells," Energy Conversion Management, Vol. 31, (1991), pp. 471-479.

[6] Garg, H. P and Adhikari, R. S. "Conventional Hybrid Photovoltaic/thermal (PV/T) Air Heating Collectors: Study-state Simulation," Renewable Energy, Vol. 11, No. 3, (1997), pp. 363-385.

[7] Hegazy, A. A. "Comparative Study of the Performances of Four Photovoltaic/thermal Solar Air Collectors," Energy Conversion Management, Vol. 41, (2000), pp. 861-881.

[8] Al-Amri, F. and Mallick, T. K. "Alleviating Operating Temperature of High Concentration Solar Cell by Active Cooling," World Renewable Energy Forum, ASES, (2012), pp. 70-74, Denver, USA.

[9] Al-Amri, F. and Mallick, T. K. "Alleviating Operating Temperature of Concentration Solar Cell by Air Active Cooling and Surface Radiation," Applied Thermal Engineering, Vol. 59, (2013), pp. 348-354.

[10] Micheli, L., Sarmah, N., Lno, X., Reddy, K. and Mallick, T. "Opportunities and Challenges in Micro- and Nano-technologies for Concentrating Photovoltaic Cooling: A Review," Renewable and Sustainable Energy Reviews, Vol. 20, (2013), pp. 595-610.

[11] Baig, H., Heasman, K. C. and Mallick, T. K. “Non-uniform Illumination in Concentrating Solar Cells,” Renewable and Sustainable Energy Reviews, Vol. 16, (2012), pp. 5890-5909.

[12] Franklin, E. and Conventry, J. “Effect of Highly Non-uniform Illumination Distribution on Electrical Performance of Solar Cell,” In Proceedings of Solar, Australian and New Zealand Solar Energy Society, 2003.

[13] Conventry, J., Franklin, E. and Blakers, A. “Thermal and Electrical Performance of a Concentrating PV/Thermal Collectors: Result from ANU CHAPS Collector,” in Proceedings of the 40th Conference of the Australia and New Zealand Solar Energy Society (ANZSES '02), Newcastle, Australia, 2002.

[14] Domenech-Garret, J. L. “Cell Behavior Under Different Non-uniform Temperature and Radiation Combined Profiles using a Two Dimensional Finite Element Model,” Solar Energy, Vol. 85, (2011), pp. 256-265.

[15] Chemisana, D. and Rosell, J. “Electrical Performance Increase of Concentrator Solar Cells under Gaussian Temperature Profiles,” Progress in Photovoltaics: Research and Applications, (2011).

[16] Al-Amri, F. and Mallick, T. “Effects of Nonuniform Incident Illumination on the ThermalPerformance of a Concentrating Triple Junction Solar Cell,” International Journal of Photoenergy, Article ID 642819, (2014).

[17] Xing, Y., Zhang, K., Zhao, J. and Han, P. "Thermal and Electrical Performance Analysis of Silica Vertical Multi-Junction Solar Cell under Non-Uniform Illumination," Renewable Energy, Vol. 90, (2016), pp. 77-82.

[18] Coney, J. E. R. and El-Shaarawi, M. A. I., “Finite Difference Analysis for Laminar Flow Heat Transfer in Concentric Annuli with Simultaneously Developing Hydrodynamic and Thermal Boundary Layers,” International Journal for Numerical Methods in Engineering, Vol. 9, (1975), pp 17-38.

[19] Al-Amri, F. G. and El-Shaarawi, M. A. I. “Combined Forced Convection and Surface Radiation Between Two Parallel Plates,” International Journal of Numerical Methods for Heat and Fluid Flow, Vol. 20, No. 2, (2010), pp. 218–239.

تأثير الاشعاع الساقط الغير منتظم على درجة حرارة خلية شمسية عالية التركيز ثلاثية الوصلات

فهد غلاب العمري

قسم الهندسة الأساسية– كلية الهندسة – جامعة الدمام

الدمام – المملكة العربية السعودية

fgalamri@uod.edu.sa

(قدم للنشر في ٢٠١٦/١٠/١٦؛ وقبل للنشر في ٢٠١٦/١٢/١)

ملخص البحث: في هذا البحث، تم تطوير نموذج عددي لايجاد درجة حرارة خلية شمسية ذات وصلات ثلاثية خاضعة لاشعاع شمسي غير منتظم عند تركيزات عالية. تتكون وحدة الخلية الضوئية من خلية شمسية ثلاثية الوصلات و مادة تلامس أمامي وغطاء زجاحي أمامي غير عاكس وصفيحة معدنية خلفية مثبتتين بالخلية الشمسية بواسطة ٠,٥مم من مادة لاصقة. تم استخدام توزيع قاوسيان لمحاكاة عدم الانتظام في الاشعاع الشمسي الساقط على الخلية، فيما تم تبريد الخلية الضوئية بواسطة الماء الجاري في القناة المثبتة خلف الخلية. ولايجاد توزيع درجات الحرارة على سطح الخلية الضوئية حلت معادلة الاستمرارية ومعادلة الزخم ومعادلة الطاقة للمائع ومعادلة الطاقة للأجزاء الصلبة باستخدام الطريقة العددية. وقد تم دراسة تأثير الانحراف المعياري لتوزيع الضوء وموقع سقوط الجزء الأكبر من الضوء ورقم رينولدز ومعامل التركيز على درجات حرارة سطح الخلية. وقد بينت النتائج أن اختلاف وعدم تماثل الضوء الساقط على سطح الخلية له تأثير كبير على درجة حرارته.